JOURNAL OF MATERIALS SCIENCE 24 (1989) 3261–3266

The nature of the dispersoids in INCONEL alloy MA6000

G. B. SCHAFFER, M. H. LORETTO, R. E. SMALLMAN
Department of Metallurgy and Materials, University of Birmingham, P.O. BOX 363, Birmingham, B15 2TT, UK

J. W. BROOKS
INCO Engineered Products Ltd, Wiggin Street, Birmingham B16 0AJ, UK

Analytical transmission electron microscopy has been used to examine the oxide dispersion in the mechanically alloyed, nickel-based, dispersion strengthened superalloy INCONEL alloy MA6000*. Four mixed Al–Y oxides were identified in consolidated powder: $Y_3Al_5O_{12}$, yttrium aluminium garnet (YAG); $YAlO_3$, yttrium aluminium perovskite (YAP); $Y_4Al_2O_9$, yttrium aluminium monoclinic (YAM), and a previously unidentified $YAlO_3$ polymorph. This new phase, designated yttrium aluminium hexagonal (YAH), has lattice parameters of $a = 2.206 \pm 0.035$ nm and $c = 3.219 \pm 0.096$ nm, a space group of $P6_3mc$ and consists of 18 close-packed oxygen layers with the yttrium and aluminium cations in the resulting interstices. It is proposed that the high local stresses, strains and temperatures which occur during the mechanical alloying process facilitate the formation of the highly complex YAH phase. All four oxide types also contain significant amounts of zirconium (up to 13 cation at %) which randomly substitutes for both the yttrium and aluminium ions. This substitution was sufficient to have caused the removal of 75% of the zirconium from solution in the matrix.

1. Introduction

Oxide dispersion strengthened (ODS) alloys derive their high-temperature strength from a uniform array of a nominally inert oxide phase in a metal matrix. The strength arises because the dispersoid provides stable and unshearable obstacles to dislocation motion. Mechanical alloying [1], is a novel process used to overcome the traditional problems associated with the manufacture of ODS nickel-base superalloys. During the mechanical alloying process, powder particles are continually welded and fractured in a high-energy ball mill until a true alloy results. The process lasts 5 to 6 days and the powders are then compacted by extrusion; the consolidated material is then hot rolled, zone annealed and given a final γ heat treatment.

INCONEL alloy MA6000 is such an alloy, designed for use as an uncooled blade material in gas turbine engines. In this alloy, as in other commercial ODS superalloys, yttria is used as the dispersoid because it is nominally inert in a metal matrix. There is, however, evidence [2–8] to show that the dispersion in the finished product consists of mixed Y–Al oxides and not Y_2O_3; the yttria is therefore not as stable as originally thought. These mixed oxides are: yttrium aluminium garnet, $Y_3Al_5O_{12}$ (YAG), yttrium aluminium perovskite, $YAlO_3$ (YAP), yttrium aluminium monoclinic, $Y_4Al_2O_9$ (YAM) and monoclinic $YAlO_3$ (YAP′). The YAG, YAP and YAM phases are well documented [9–11] and are shown as congruently melting phases in the pseudo-binary Y_2O_3–Al_2O_3 phase diagram [12]. There is also another $YAlO_3$ phase [13], grown by a precipitation technique, which is not included in the phase diagram, not has it been identified in an ODS alloy. This phase has a hexagonal structure of space group $P6_3/mmc$ with lattice parameters of $a = 0.3678$, $c = 1.052$ nm and $c/a = 2.86$. There are two formula units per unit cell. The structure has a six-layer oxygen stacking sequence with yttrium in eight- and aluminium in five-fold coordination.

The precise nature of all the oxides in commercial ODS superalloys is not known, nor has any significant work been done to date on the formation of these mixed oxides during mechanical alloying, their proportions in the finished product or on their stability at service temperatures. This work is therefore an analysis of the crystal chemistry of the oxide dispersoid in consolidated MA6000 powder. The changes which occur in the oxides during the subsequent manufacturing stages and their stability at service temperatures will be reported elsewhere.

2. Experimental details

The yttria starting powder and compacted (extruded) MA6000 were obtained from Inco Engineered Products Ltd. The nominal composition of the alloy is (wt %). 15Cr–2Mo–4W–4.5Al–2.5Ti–2Ta–0.05C–0.01B–0.15Zr–1.1Y_2O_3–bal Ni. The oxides in MA6000 were extracted on to carbon replicas in the normal

---

*INCONEL is a registered trademark of the Inco Family of companies.

0022–2461/89 $03.00 + .12

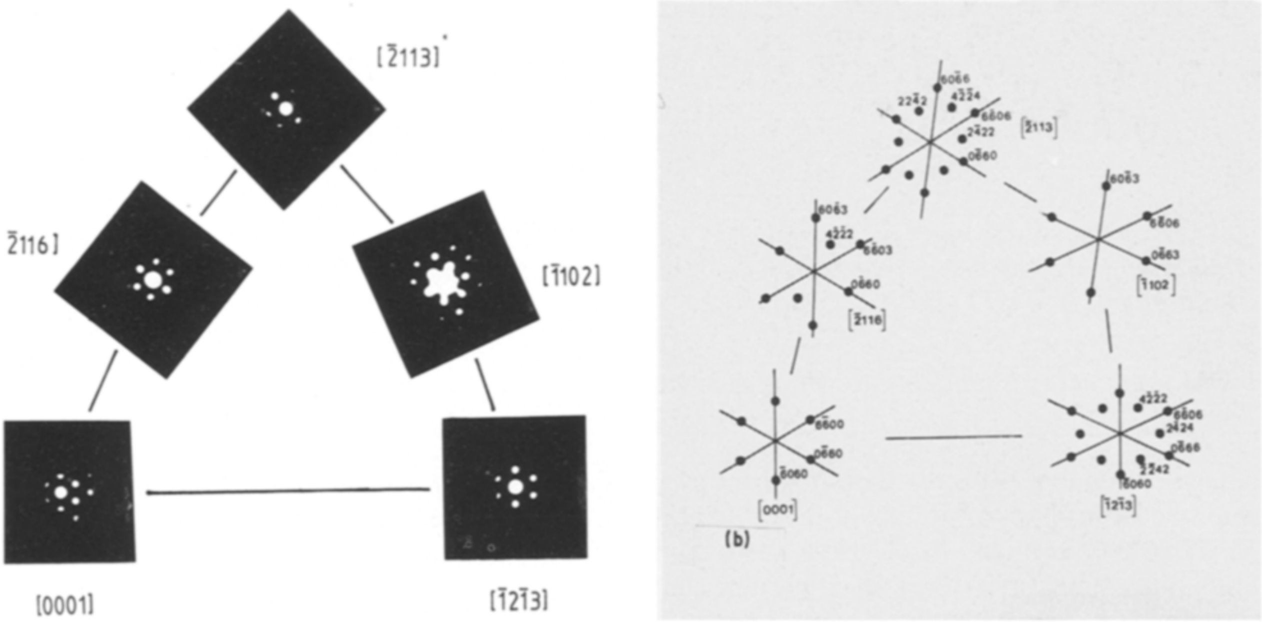

Figure 1 (a) Zone axis pattern map for YAH. (b) Indexed schematic drawing of (a).

manner. Samples were electropolished in a 12% perchloric acid/ethanol solution prior to carbon deposition and the replica was removed by electroetching in a solution of 6% perchloric acid in acetic acid; both processes used a current density of approximately $0.1\,\mathrm{A\,mm^{-2}}$. Particles of the yttria powder were suspended in methanol and lifted off on to carbon support films. The replicas were examined by analytical TEM in a Philips EM400T and a Jeol 4000FX. To characterize the oxides, zone axis pattern (ZAP) maps were constructed and the Al/Y concentration measured for each particle examined. Where appropriate, convergent beam electron diffraction (CBED) was used to determine the crystal space group.

3. Results

The starting powder was confirmed to be the cubic form of Y_2O_3; there were no detectable contaminants. In the consolidated material, the oxides were all spherical and ranged in diameter from 10 to 120 nm. Four different oxide types were identified: YAG, YAP and YAM and a previously unidentified Y–Al polymorph. The YAG, YAP and YAM oxides occurred in approximately equal proportions and accounted for half the dispersoid. Neither Y_2O_3 nor the YAP′ phase were identified.

The fourth type of particle had the same Al/Y ratio as the YAP phase and thin-window energy dispersive spectrometry (EDS), showed it to be an oxide, but it had a hexagonal crystal structure which did not correspond to any of the phases reported in earlier work. A microdiffraction ZAP map taken from one of these particles (designated yttrium aluminium hexagonal, YAH) and an associated schematic ZAP map are shown in Fig. 1. The symmetry of the first order Laue zone in $[0\,0\,0\,1]$, together with controlled tilting experiments, confirmed the hexagonal nature of the phase. A CBED analysis was used to characterize further this phase (Fig. 2): the symmetry of the zero order layer and the symmetry of the whole pattern of the $[0\,0\,0\,1]$ zone axis are both 6 mm and the possible diffraction groups are therefore 6 mm and $6\mathrm{mm}1_R$. The corresponding symmetries in the $[\bar{1}\,1\,0\,2]$ zone axis are both m and the possible diffraction groups are therefore m and $\mathrm{m}1_R$. No higher order Laue zones (HOLZ) lines are visible in the zero order disc and it is therefore not possible to distinguish which of these two diffraction groups applies to this orientation; but fortunately this does not hinder the point group determination for this particular phase. If the diffraction group for the $[0\,0\,0\,1]$ pole is $6\mathrm{mm}1_R$, then the point group is 6/mmm, but as this does not correspond to a possible point group derived from the $[\bar{1}\,1\,0\,2]$ zone axis whether its diffraction group is m or $\mathrm{m}1_R$, it cannot be the point group of the phase. If the diffraction group of the $[0\,0\,0\,1]$ pole is 6 mm, then the point group is 6 mm. As this is only common point group if the diffraction group of the $[\bar{1}\,1\,0\,2]$ pole is either m or $\mathrm{m}1_R$, it must be the point group of the phase.

The YAH phase could therefore have one of four possible space groups: P6mm, P6cc, $P6_3cm$ and $P6_3mc$. For the P6cc and $P6_3cm$ space groups, the $h\bar{h}0l$ reflection occurs only when $l = 2n$ [14]. The presence of $6\,0\,\bar{6}\,3$ diffraction maxima in $\langle 1\,\bar{1}\,0\,2\rangle$, which were not due to double diffraction, therefore eliminated P6cc and $P6_3cm$ as possible space groups for this phase. There are no conditions limiting possible reflections in P6mm and all the possible limiting conditions are satisfied for $P6_3mc$. The occurrence of $0\,0\,0\,3$ diffraction maxima in $[1\,\bar{2}\,1\,0]$ due to double diffraction implies that there is a glide plane and/or a screw axis present. As P6mm has neither a glide plane nor a screw axis, it cannot be the space group of the phase. The space group of the YAH oxide is therefore $P6_3mc$.

Measurements of calibrated microdiffraction patterns from seven different particles gave the lattice parameters of the phase as: $a = 2.206 \pm 0.035$ nm, $c = 3.219 \pm 0.096$ nm and $c/a = 1.46$. These lattice

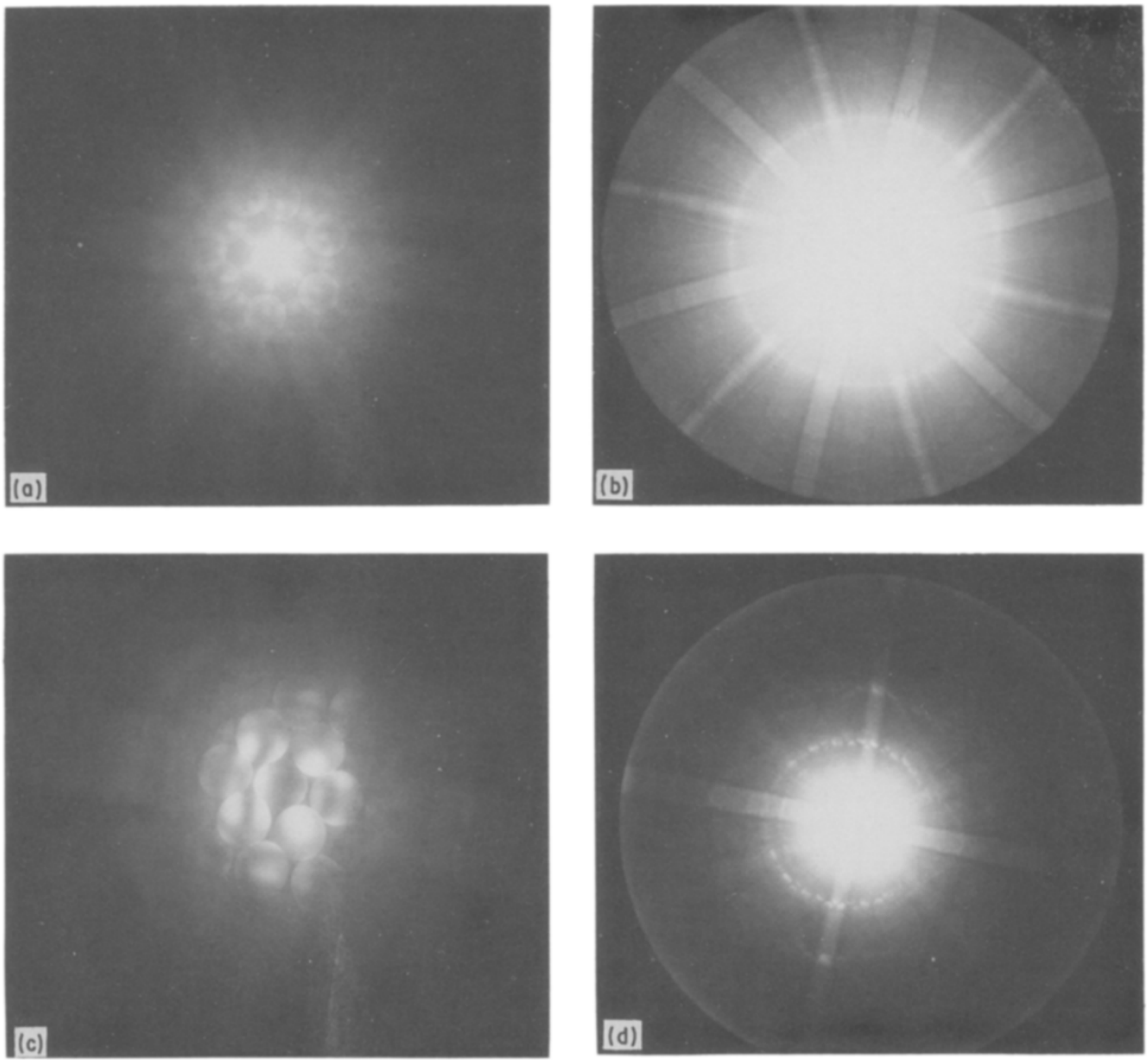

Figure 2 Convergent beam electron diffraction patterns of a YAH particle. (a) Zero order layer of $[0001]$, symmetry 6 mm. (b)Whole pattern of $[0001]$, symmetry 6 mm. (c) Zero order layer of $[\bar{1}102]$, symmetry m. (d) Whole pattern of $[\bar{1}102]$, symmetry m.

parameters were confirmed by measurements of the HOLZ in $[0001]$ and $[10\bar{1}0]$ CBED patterns and by the measurement of basal plane lattice fringes.

In addition to aluminium and yttrium, all the oxides also contained zirconium, between 0.2 ± 0.1 and 13.5 ± 0.5 cation at %. A typical EDS spectrum is shown in Fig. 3. The presence of zirconium is irrefutable; there were no other contaminants. All the oxides deviated randomly from stoichiometry. There was no consistent excess of either aluminium or yttrium, nor was there a consistent variation in zirconium content with aluminium or yttrium concentration (cf Fig. 4).

4. Discussion

This work has confirmed that yttria does not occur in MA6000, but that it had transformed during the early stages of manufacture to a number of mixed Y–Al oxides. During the course of this work, two unexpected facts have been revealed: (1) a previously unidentified oxide accounts for half the dispersoid, and (2) all the oxides contain substantial amounts of zirconium. The structure of the YAH phase, the zirconium contamination and how the formation of the YAH phase is dependent on the mechanical alloying process itself, will be discussed in turn.

4.1. The YAH oxide

Because the YAH oxides studied here were small spheres embedded in a superalloy matrix, single-crystal X-ray data were not obtainable and atomic coordinates cannot therefore be determined. A more complete model of the structure than that given by the space group and lattice parameters can, however, be constructed, by comparing it with other similar compounds. There are six other hexagonal variants of the ABO_3-type compounds (Table I), although none of these has the same space group as the YAH phase. Of these six phases, $BaTiO_3$ and $BaNiO_3$ can be excluded as possible models for the YAH phase, because they consist of close packed BaO_3 layers with the Ba^{2+} ion in 12-fold coordination. The Ba^{2+} ion is approximately 60% bigger than the Y^{3+} ion, which is too small for cuboctahedron coordination: the Y/O radius is ≈ 0.8 compared with a minimum ratio of 1 for 12-coordination. The other four compounds all consist

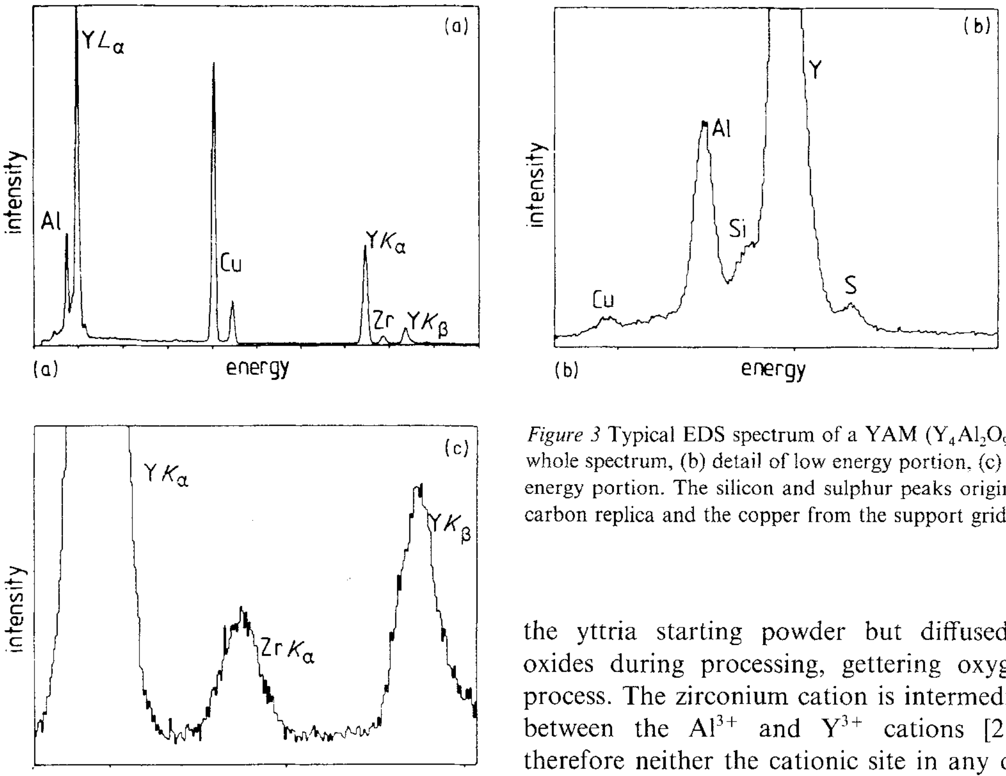

Figure 3 Typical EDS spectrum of a YAM ($Y_4Al_2O_9$) particle. (a) whole spectrum, (b) detail of low energy portion, (c) detail of high energy portion. The silicon and sulphur peaks originate from the carbon replica and the copper from the support grid.

of six close packed (or eutactic) oxygen layers with the cations in the interstices. The *c* lattice parameter for the YAH phase is 3.06 times that of the $YAlO_3$ phase of Bertaut and Mareschal [13]. The $YMnO_3$, $YGaO_3$ and $InGaO_3$ phases have similar *c* lattice parameters to this $YAlO_3$ phase, because in these cases, this is primarily determined by the oxygen stacking. It therefore seems probable that the YAH phase consists of 18 close packed oxygen layers with the metal cations in the resulting interstices.

4.2. Zirconium

The zirconium contamination did not arise from the yttria starting powder but diffused into the oxides during processing, gettering oxygen in the process. The zirconium cation is intermediate in size between the Al^{3+} and Y^{3+} cations [21–24] and therefore neither the cationic site in any of the four oxide types would be particularly favoured by the Zr^{4+} ion. If the Zr^{4+} ion substituted for either Y^{3+} or Al^{3+}, there would be the concomitant creation of vacancies in order to maintain electrical neutrality. If, for example, the zirconium substituted for yttrium, then for every three Zr^{4+} ions entering the lattice, four Y^{3+} ions would be ejected with the creation of one vacancy. The resulting structure would be non-stoichiometric with a molecular formula for YAP (or YAH) of $Y_{n-4x}Al_nZr_{3x}V_xO_{3n}$ for $n \gg x$. The Al to Y + Zr ratio should then increase with increasing zirconium content. The points derived on the assumption that the Zr^{4+} ion substitutes for Y^{3+}, together with the observed values for the YAH phase, are plotted on Fig. 4. Similar results are obtained if it is assumed that Zr^{4+} substitutes for Al^{3+}. It therefore appears that the Zr^{4+} cation randomly substitutes for both the yttrium and aluminium cations. Because the Zr^{4+} ion is intermediate in size between the Y^{3+} and Al^{3+} ions, the octahedral sites would expand due to the replacement of Al^{3+} with Zr^{4+} while the dodecahedral sites would decrease in size as Y^{3+} was replaced by Zr^{4+}. The expansion of the one site would then be compensated for by a decrease in the other with a corresponding decrease in the lattice distortions. It is therefore reasonable that both cationic sites are occupied by Zr^{4+}. This random substitution is in contrast to previous work on mixed rare earth oxides where Zr^{4+} was found to substitute for Al^{3+} [25] and where Zr^{3+} replaced Y^{3+} [26].

TABLE I The hexagonal variants of the ABO_3 compounds

Compound	Lattice parameter (nm)	Space group	Reference
$BaTiO_3$	$a = 0.5735$ $c = 1.401$ $c/a = 0.244$	$P6_3/mmc$	[15]
$BaNiO_3$	$a = 0.5629$ $c = 0.4811$ $c/a = 0.085$	$P6_3/mmc$	[16]
	$a = 0.5580$ $c = 0.4832$ $c/a = 0.087$	$P6_3mc$	[17]
$YMnO_3$	$a = 0.6125$ $c = 1.141$ $c/a = 0.186$	$P6_3cm$ or $P3cl$	[18]
$TGaO_3$	$a = 0.6065$ $c = 1.1615$ $c/a = 0.192$	$P6_3cm$	[19]
$InGaO_3$	$a = 0.3310$ $c = 1.2035$ $c/a = 0.364$	$P6_3/mmc$	[20]
$YAlO_3$	$a = 0.3678$ $c = 1.052$ $c/a = 0.286$	$P6_3/mmc$	[13]

As zirconium is added to the structure to improve the stress rupture life and ductility [27], its removal from the matrix would presumably cause a decrease in the alloy's mechanical properties. In the finished product, approximately 75% of the zirconium which was added to the alloy is tied up in the oxide [28]. This depletion presumably has a significant influence on the mechancial properties. This effect is currently being investigated.

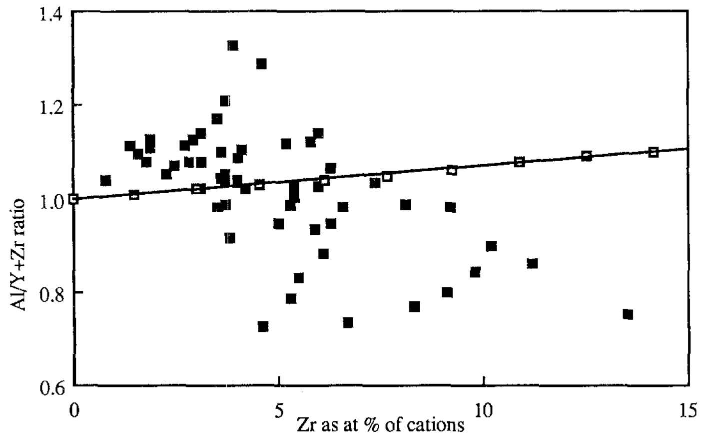

Figure 4 The Al/Y + Zr ratio as a function of the zirconium content showing that the Zr^{4+} ion does not directly substitute for the Y^{3+} ion. (■) Experimental, (□) theoretical.

4.3. The formation of the YAH oxide

It is most likely that the formation of the mixed oxides, and in particular the YAH phase, occurred during the mechanical alloying process itself and not during consolidation by extrusion. During milling, very high local stresses, strains and temperatures prevail and these continue for 5 to 6 days and it is therefore likely that the major structural and chemical changes would have occurred in the oxides in this time. Mechanical alloying would facilitate the formation of the YAH phase in a number of ways. The rate, k, of a chemical reaction is given by the Arrhenius equation

$$k = A\,e^{-E/RT}$$

where A is the pre-exponential factor, E the activation energy, R the universal gas constant and T the temperature. The activation energy is a measure of the amount of energy required to form an activated complex (the species which corresponds to the maximum energy stage in the reaction process). The YAH phase is highly ordered with a big unit cell and because it has a complex structure it is likely to have a higher activation energy of formation than the other Y/Al mixed oxides. The high temperatures and pressures provided by the milling cycle will supply the additional energy necessary to surmount this activation energy barrier. The pre-exponential factor in the Arrhenius rate equation is the probability that the molecules are in the required energy state and it is a function of the collision energy of the reactant molecules which depends on the number of contacts between reactants and on their kinetic, rotational and vibrational energies. Not only will the temperatures and stresses of mechanical alloying increase the collision energy of the reactants, but the large strains imposed by mechanical alloying will increase the number of defects in the oxides, hence diffusion rates and collision frequencies will also increase. Mechanical alloying therefore provides, simultaneously, high stresses and strains and temperatures which together increase the reaction rate, thus enabling the stable YAH phase to form. It is therefore probable that the YAH phase can form only during mechanical alloying. That the YAH phase has not been found in previous studies of the Y_2O_3–Al_2O_3 pseudo-binary system is therefore not surprising because only high temperatures and static pressures were used to generate these oxides. To test this hypothesis, it will be necessary to mechanically alloy yttria and alumina and to examine the resulting phases. This may prove a feasible route for the manufacture of single YAH crystals which could then be used to determine the crystal structure.

5. Conclusions

1. Yttria does not occur in MA6000. Although it was used as a raw material, it had transformed during mechanical alloying into four mixed Y–Al oxides. These are: $Y_3Al_5O_{12}$, yttrium aluminium garnet, YAG; $YAlO_3$, yttrium aluminium perovskite, YAP; $Y_4Al_2O_9$, yttrium aluminium monoclinic, YAM; and a previously unreported $YAlO_3$ phase, here designated yttrium aluminium hexagonal, YAH.
2. This YAH phase, space group $P6_3mc$, has lattice parameters of $a = 2.206 \pm 0.035$ nm and $c = 3.219 \pm 0.096$ nm. Its structure can be visualized as consisting of 18 eutectic oxygen layers with the yttrium and aluminium in the resulting interstices.
3. All four oxide phases contain zirconium which randomly substitutes for both the yttrium and aluminium cations. The bulk of the zirconium addition is tied up in the oxides; only 25% remains in the matrix.

Acknowledgements

G.B.S. acknowledges the Committee of Vice-Chancellors and Principals for financial support in the form of an Overseas Research Studentship.

References

1. J. S. BENJAMIN, *Met. Trans.* **1** (1970) 2943.
2. J. S. BENJAMIN, T. E. VOLIN and J. H. WEBER, *High Temp. High Press.* **6** (1974) 443.
3. R. E. LAWN, F. G. WILSON and C. D. DESFORGES, *Powder Metall.* **19** (1976) 196.
4. F. G. WILSON, B. R. KNOTT and C. D. DESFORGES, *Met. Trans. A.* **9A** (1978) 275.
5. J. J. FISCHER, I. ASTLEY and J. P. MORSE, in "Superalloys 76" Proceedings of a Conference, Seven Springs, Pennsylvania, September 1976, edited by B. H. Kear, T. Muzyka, S. Tien and V. Wlodik (Claitors, Baton Rouge, Louisiana, 1976) p. 76.
6. M. RAGHAVAN, C. KLEIN and R. PETKOVIC-LUTON, in "Thirty-ninth Annual EMSA Meeting", edited by G. W. Bailey, (1981) p. 142.
7. M. RAGAHVAN, J. W. STEEDS and R. PETKOVIC-LUTON, *Met. Trans. A* **13A** (1982) 953.
8. S. K. KANG and R. C. BENN, *ibid.* **16A** (1985) 1285.

9. H. S. YODER and M. L. KEITH, *Amer. Mineral.* **36** (1951) 519.
10. S. GELLER and E. A. WOOD, *Acta Crystallogr* **9** (1956) 563.
11. I. WARSHAW and R. ROY, *J. Amer. Ceramic. Soc.* **42** (1959) 434.
12. J. S. ABELL, I. R. HARRIS, B. COCKAYNE and B. LENT, *J. Mater. Sci.* **9** (1974) 527.
13. F. BERTAUT and J. MARESCHAL, *Compt. Rend.* **257** (1963) 867.
14. "International Tables for X-Ray Crystallography", Vol. 1 (The Kynock Press, Birmingham, 1969.
15. R. D. BURBANK and H. J. EVANS Jr, *Acta Crystallogr* **1** (1948) 330.
16. Y. TAKEDA, F. KANAMARU, M. SHIMIDA and M. KOIZUMI, *ibid.* **B32** (1976) 2464.
17. J. J. LANDER, *ibid.* **4** (1951) 148.
18. H. L. YAKEL, W. C. KOEHLER, F. BERTAUT and E. F. FORRAT, *ibid.* **16** (1963) 957.
19. S. GELLER, J. B. JEFFRIES and P. J. CURLANDER, *ibid.* **B31** (1975) 2770.
20. R. D. SHANNON and C. T. PREWITT, *J. Inorg. Nucl. Chem.* **30** (1968) 1389.
21. V. M. GOLDSCHMIDT, T. BARTH, G. LUNDE and W. H. ZACHARIASEN, *Skr. norske Vidensk. Akad. I, Mat.-Nat. Kl. No, 2,* **1926**.
22. R. D. SHANNON and C. D. PREWITT, *Acta Crystallogr.* **B25** (1969) 925.
23. *Idem. ibid.* **B26** (1970) 1046.
24. R. D. SHANNON, *ibid.* **A32** (1976) 751.
25. D. MATEIKA, R. LAURIEN and Ch. RUSCHE, *J. Crystal Growth* **56** (1982) 677.
26. H. R. ASATRYAN, A. S. KUZANYAN, A. G. PETROSYAN and E. J. SHAROYAN, *Phys. Status Solidi B* **135** (1986) 343.
27. R. T. HOLT and W. WALLACE, *Int. Met. Rev.* **3** (1976) 1.
28. G. B. SCHAFFER, PhD thesis, University of Birmingham (1988).

Received 18 July
and accepted 21 November 1988